Letter Vol. 42, No. 20 / October 15 2017 / Optics Letters 4083

Optics Letters

Arbitrary-shaped Brillouin microwave photonic filter by manipulating a directly modulated pump

WEI WEI,[1,2] LILIN YI,[1,*] YVES JAOUËN,[2] AND WEISHENG HU[1]

[1]State Key Lab of Advanced Optical Communication Systems and Networks, Shanghai Institute for Advanced Communication and Data Science, Shanghai Jiao Tong University, Shanghai 200240, China
[2]LTCI, Télécom ParisTech, Université Paris Saclay, Paris 75634, France
*Corresponding author: lilinyi@sjtu.edu.cn

Received 18 August 2017; revised 8 September 2017; accepted 12 September 2017; posted 13 September 2017 (Doc. ID 305090); published 4 October 2017

We present a cost-effective gigahertz-wide arbitrary-shaped microwave photonic filter based on stimulated Brillouin scattering in fiber using a directly modulated laser (DML). After analyzing the relationship between the spectral power density and the modulation current of the DML, we manage to precisely adjust the optical spectrum of the DML, thereby controlling the Brillouin filter response arbitrarily for the first time, to the best of our knowledge. The filter performance is evaluated by amplifying a 500 Mb/s non-return-to-zero on-off keying signal using a 1 GHz rectangular filter. The comparison between the proposed DML approach and the previous approach adopting a complex IQ modulator shows similar filter flexibility, shape fidelity, and noise performance, proving that the DML-based Brillouin filter technique is a cost-effective and valid solution for microwave photonic applications.

OCIS codes: (060.5625) Radio frequency photonics; (290.5900) Scattering, stimulated Brillouin; (060.2330) Fiber optics communications.

https://doi.org/10.1364/OL.42.004083

As a core microwave photonic component, the microwave photonic filter (MPF) has attracted consistent interest due to its prominent superiority in tunability and reconfigurability [1,2]. The realization of the MPF can be roughly categorized into two main approaches: one type is delayed-tap-based finite impulse response filter in time domain [3]; the other one is based on optical filtering techniques to filter the optical signal modulated by the radio-frequency signal in the frequency domain [4]. For both approaches, the research trend is always to increase the flexibility while decreasing the cost.

Stimulated Brillouin scattering (SBS) is used for realizing MPFs, thanks to its high selective amplification or absorption [5–9]. The filter bandwidth can be broadened equivalently by using either a multi-tone pump with a spacing less than the natural Brillouin linewidth or a fast-frequency swept pump. Previously, we have realized an arbitrary-shaped software-defined MPF with ~15-MHz configurable resolution based on the SBS effect in fiber, and we compared it with different techniques in terms of filter control precision, frequency tuning range, and filter selectivity [9]. An accurate Brillouin pump spectral control scheme has been demonstrated utilizing single sideband modulation to map the designed electrical spectrum onto the optical domain. However, this approach required an IQ modulator (IQM) with accurate bias control and a 90 deg hybrid coupler. In addition, a digital-to-analog converter (DAC) with a high sampling rate was necessary, which further increased the cost. A directly modulated laser (DML) is a component widely used in cost-sensitive scenarios. By adjusting the modulation current, the optical spectrum of the DML can be controlled to some extent [10,11]. However, the precise control of the DML spectrum can be very difficult.

In this Letter, we present the capability of precisely and arbitrarily controlling the shape of MPFs by using a low-cost DML. The designed modulation current is generated by a DAC with only 1 GS/s sampling rate and is adjusted accurately with an effective feedback algorithm. Rectangular MPFs with bandwidths from 500 MHz to 2 GHz are realized. MPFs with arbitrary shapes such as truncated Gaussian, super Gaussian, triangular, and their inverse shapes are also obtained. The filter performance of the proposed DML approach and the previous IQM approach has been evaluated by amplifying a 500 Mb/s non-return-to-zero on–off keying (NRZ-OOK) signal. The DML-based approach proves to have similar filter flexibility, shape fidelity, and noise performance, but with far lower complexity, which is preferable in cost-sensitive scenarios.

It is well-known that the current modulation of a DML not only results in an intensity modulation (IM), but also gives rise to a modulation of carrier density which, in turn, changes the frequency of the output light [12]. Different from the external modulation, the DML enables a considerable spectrum broadening by using an electrical signal with large amplitude instead of a large bandwidth, which reduces the requirement of the signal generation. By using a broadened DML as a Brillouin pump, the effective Brillouin gain spectrum can be expressed as the convolution of the natural Brillouin gain with a broadened DML spectrum [13]:

$$G_B(f) = \exp\{[g_B(f) * S_P(f + \Omega_B/2\pi)]L_{\text{eff}}\}, \quad (1)$$

where $G_B(f)$ is the gain of the signal, L_{eff} is the effective fiber length, $g_B(f)$ is the natural Brillouin gain, and $S_p(f + \Omega_B/2\pi)$

is the power spectrum of the pump source. Note that the Brillouin gain has a downward shift of Ω_B. If the pump bandwidth is much larger than the natural linewidth of the Brillouin gain, the gain of the signal in the unit of decibels can be approximated by [10]

$$\log[G_B(f)] \propto S_P(f + \Omega_B/2\pi). \quad (2)$$

We then use a simplified estimation to deduct the relationship between the filter shape and the modulation current of the DML. Under a slowly varying small signal condition, IM and frequency modulation (FM) transfer functions can be considered. We can use a constant C_i (mW/mA) to describe the relationship between the output power variation and the modulation current. At relatively low modulation frequency (<1 GHz), we can use a constant C_f (MHz/mA) to describe the linear relationship between the frequency chirp and the modulation current where adiabatic chirp is dominant and the transient chirp can be neglected [14]. The constant C_f here can be seen as spectrum broadening efficiency. It implies that a specific modulation current corresponds to a unique output frequency, and the optical power spectral density of the DML accords with the temporal distribution of the modulation current value. After discretization, it is obvious that the optical power at a specific frequency is proportional to the time duration for which the current stays at the corresponding value

$$S_P(f_i) \propto \Delta t(I_{f_i}). \quad (3)$$

Combining Eqs. (2) and (3), we finally get

$$\log[G_B(f)] \propto \Delta t(I_{f+\Omega_B/2\pi}), \quad (4)$$

which indicates that the Brillouin gain at a specific frequency in the unit of decibels has a linear relationship with the time duration of the current waveform at the corresponding value. This deduction is the foundation of the filter shape design and control. For simplicity, this estimation does not take into account the thermal effect.

The filter control mechanism is composed of two parts: the pre-design of the current waveform and accurate feedback adjustment. We first use Eq. (4) to design the waveform according to the targeted filter shape. As sketched in Fig. 1, a linear ramp is needed for a rectangular filter and a parabolic ramp for a triangular filter. Here we use a non-periodic ramp to make the laser spectrum continuous, thus avoiding unwanted peaks within the Brillouin gain. The average duration of the ramps is set to 10 ns so that only the adiabatic chirp is dominant. Meanwhile, 10 ns is far smaller than the signal transmission time through the fiber (~60 μs for a 12.5 km fiber), making the swept pump equivalent to a broadband pump.

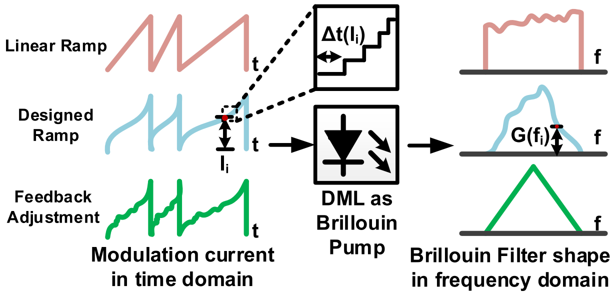

Fig. 1. Sketch of generating a triangular filter by adjusting the modulation current of a DML as a Brillouin pump.

Due to the unconsidered IM modulation and weakly nonlinear FM modulation induced by the thermal chirp [15], the designed waveform usually leads to an MPF with a non-ideal shape. Thus, we propose a feedback algorithm for a more accurate adjustment of the filter shape. We first measure the filter shape by using an electrical vector network analyzer (EVNA). Then we calculate the new time duration Δt_{n+1} for each frequency component of the filter based on the relationship between the Brillouin gain and the previous time duration Δt_n of the corresponding current I_i:

$$\Delta t_{n+1}(I_i) = \Delta t_n(I_i)\left(1 - F_e \frac{G_M(f_i) - G_T(f_i)}{G_M(f_i)}\right), \quad (5)$$

where G_M and G_T are the measured and targeted gain at frequency f_i, and F_e is an empirical factor for controlling the convergence speed. After merely 3–7 iterations (related to the shape precision) of the feedback adjustment, the pump waveform for the targeted shape can be obtained and this optimal waveform can be stored for future use with no need for further feedback. It should be noted that the amplitude of the modulation current defines the bandwidth of the MPF, which can be reconfigured. The central frequency of the proposed MPF can be easily changed by changing the wavelength of the DML through the bias current or temperature. Thus, the proposed MPF provides flexibility on the bandwidth, central frequency and, most importantly, the filter shape at the same time.

We simulate this process with configurations mentioned above. In the simulation, we set C_i to 0.24 mW/mA and C_f to 250 MHz/mA according to the specific laser we use. Figure 2 shows the designed waveforms and the corresponding rectangular and triangular filter shapes before and after feedback adjustment. The rectangular and triangular filters obviously have better shape fidelity after the accurate feedback adjustment. We also compare our simplified model with the model using full coupled rate equations which describe the relationship of the carrier density, the photon density, and the optical phase [12,16]. The two models result in similar filter shapes, validating our linear approximation under slowly varying small signal modulation. Meanwhile, the simplified model is also time efficient compared with the rate equation model where the time-consuming integration is needed for obtaining accurate numerical solutions.

Then we conduct the experiment adopting a DML-based pump and compare the shape fidelity and performance with the IQM approach. The experimental setup is shown in Fig. 3. In the DML pump branch, a DML is driven by a well-designed current waveform generated with a 1 GS/s DAC. After being boosted by an erbium-doped fiber amplifier, the modulated

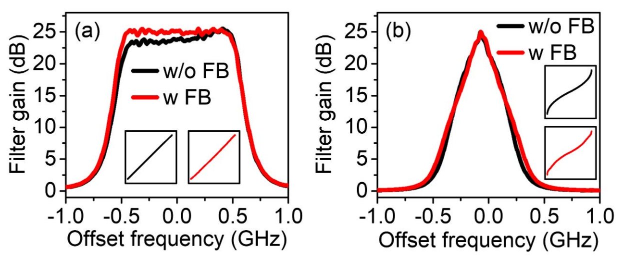

Fig. 2. Simulation results of the designed waveforms and the corresponding filter shapes for (a) rectangular and (b) triangular cases before and after feedback adjustment.

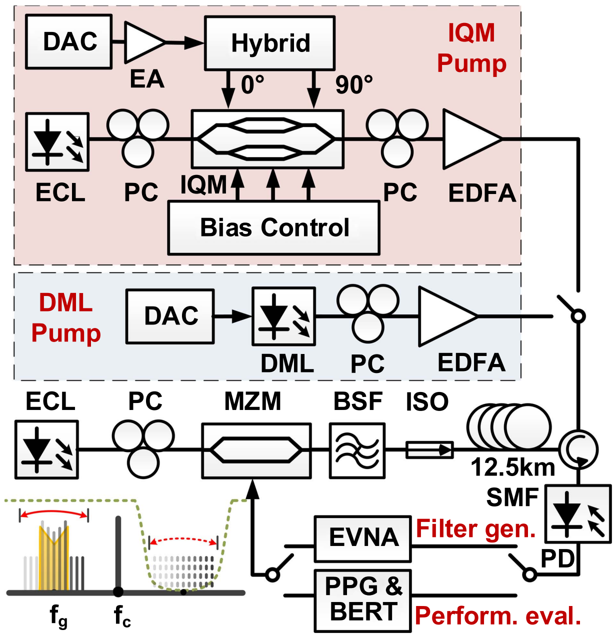

Fig. 3. Experimental setup for generating and evaluating the arbitrary-shaped filters with both DML and IQM approaches.

light is sent into a 12.5 km single-mode fiber (SMF) acting as the Brillouin pump. A polarization controller is used to maintain the SBS gain at the maximum value. As long as the pump and the probe signal are both single-polarized, this simple control can ensure the constant and stable gain. An alternative solution is to use a depolarized pump to make the SBS gain polarization insensitive [8]. In the probe branch, a swept signal covering the whole SBS gain region is generated by an EVNA. It modulates the continuous-wave light in a Mach–Zehnder modulator to generate the probe signal. After suppression of the high-frequency sideband by a narrow optical bandstop filter, the probe light propagates through the fiber and is amplified when it sweeps within the SBS gain region, as shown in the inset. Then the probe signal is detected by a photodiode (PD) and is sent to the EVNA, where the amplitude and phase response are measured. The SBS gain spectra are obtained by comparing the results when the SBS pump is on and off.

First, we demonstrate rectangular filters with tunable bandwidths using the DML approach. The filter bandwidth is easily reconfigured from 500 MHz to 2 GHz by changing the DAC output voltage from ~0.1 to ~0.4 V which can be easily reached for most of the DACs. The bandwidth broadening efficiency here is ~5 GHz/V. The pump power is set to 18.0, 20.2, and 23.0 dBm for 500 MHz and 1 and 2 GHz filters, respectively. As shown in Fig. 4, all the amplitude responses of the filters have steep edges and flat passbands. The filter selectivity demonstrated here is ~25 dB, but it can be further increased to more than 50 dB when multi-stage amplification is adopted [8]. The passband ripple is controlled within 1.5 dB, leading to smooth phase responses. The original filter shape without feedback adjustment is also given in the inset, showing the validity of the feedback algorithm. Although the sampling rate of the DAC is set to merely 1 GS/s, the filter bandwidth reaches 2 GHz and can be further extended by increasing the amplitude of the modulation current and the pump power,

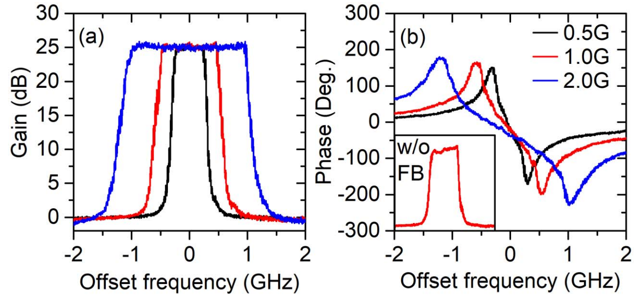

Fig. 4. (a) Amplitude and (b) phase response of rectangular MPFs using the DML approach with different bandwidths. The inset in (b) shows the 1 GHz DML-based filter without feedback adjustment.

which is limited theoretically by the Brillouin frequency shift of ~11 GHz in fiber.

The filter shape can be defined precisely, manifesting the advantage of the proposed approach. By using well-designed current waveforms and applying the feedback adjustment according to the targeted filter shape, the final MPF shapes are obtained with high fidelity, as shown in Fig. 5, including truncated Gaussian, super-Gaussian, triangular, and their inverse shapes with a 1 GHz bandwidth. The corresponding phase responses are dependent on the specific filter amplitude responses. The modulation current for each filter shape is demonstrated in the insets. The adjustment of the feedback process is elaborate and inconspicuous which, in turn, proves its high accuracy. The arbitrary-shaped filter can be used for high-resolution electrical or optical signal processing such as reshaping the pulse [9]. It should be noted that the control precision of the filter shape is also related to the stability of the DML laser. The DML should be locked to the signal laser by opto-electronic feedback or other methods if high shape fidelity is required [17].

We then compare the rectangular filter generated by the DML approach with the IQM approach. The IQM pump

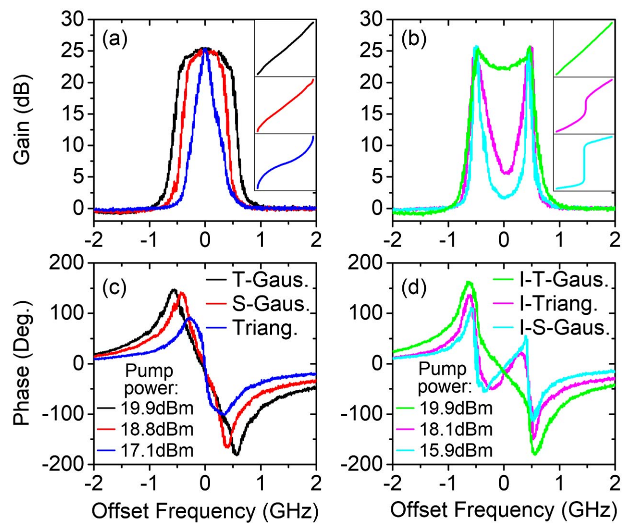

Fig. 5. (a), (b) Amplitude and (c), (d) phase response of arbitrary-shaped MPFs using a DML with a pre-designed waveform and feedback adjustment. The insets are the corresponding current waveforms. T, truncated; Gaus., Gaussian; S, super; Triang., triangular; I, inverse.

setup is shown in Fig. 3. A 10 GS/s DAC with a high-gain electrical amplifier is used to generate the multi-tone electrical waveform. The high sampling rate ensures precise filter shape control resulting in better performance. After being split into two branches with a 90 deg difference in an electrical hybrid, the waveform modulates the light of an external cavity laser in the IQM. An accurate bias control system is required to maintain the IQM at the state of carrier suppressed single sideband modulation. It is evident that the IQM approach with all the peripheral components is more complex and expensive than the DML approach with cost-efficient control circuits and a low sampling rate DAC. The filter shape comparison is shown in Fig. 6. The DML approach results in a similar passband ripple and slightly less steep edges which leads to smaller phase variation at two filter edges. For most applications, this minor shape degradation is acceptable; in addition, the DML method greatly simplifies the setups.

We further compare the performance of the filters in amplifying NRZ-OOK signals. The experimental setup has been shown in Fig. 3 adopting a pulse pattern generator and a bit error rate (BER) tester in place of the EVNA. The rectangular filters are generated using both DML and IQM methods with a 25 dB gain and 1 GHz bandwidth, which have been shown in Fig. 6. The bit rate of the signal is set to 500 Mb/s so that the main lobe of the signal covers the whole Brillouin gain region of 1 GHz. The signal power injected into the SMF is set to −20 dBm when evaluating the filter performance and is increased to −10 dBm, ensuring enough received power at the PD when measuring the original case without filter. The relationship between the BER and the received power of the PD is shown in Fig. 7. At a BER close to 10^{-3}, the presence of rectangular filters does not induce obvious penalty. With the increase of the received power, the penalty increases from ∼1.5 dB at a BER of 10^{-6} to ∼5 dB at a BER of 10^{-9} due to the spontaneous Brillouin emission [18]. However, if taking into account the 25 dB gain that the filter induces, the power budget is even increased by at least ∼20 dB at a BER of 10^{-9}. The eye diagrams also indicate that the performance difference between these two approaches is indistinctive. Thus, the DML approach with merely 1 GS/s DAC has almost the same performance as the IQM approach adopting 10 GS/s DAC.

In summary, we have presented a cost-effective gigahertz-wide arbitrary-shaped MPF solution. Instead of using a complicated IQM setup and high sampling rate DAC, we use merely a DML and a 1 GS/s DAC, but achieve similar performance. With a well-designed current waveform and accurate feedback adjustment, the filter shape has been arbitrarily controlled with high shape fidelity. The comparison between the proposed DML approach and the previous IQM method shows that the two solutions result in similar filter shapes and indistinctive noise performance. The DML approach has a much simpler structure and lower requirements for the DAC while still keeping flexibility in the filter bandwidth, filter center frequency, and most of all the arbitrary configured shape, which is more suitable for cost-sensitive microwave photonic or optical applications. It paves the road to realizing compact MPFs and integrated instruments. Meanwhile, the proposed spectrum tailoring technique can also be used for other scenarios where high-precision DML output is desirable.

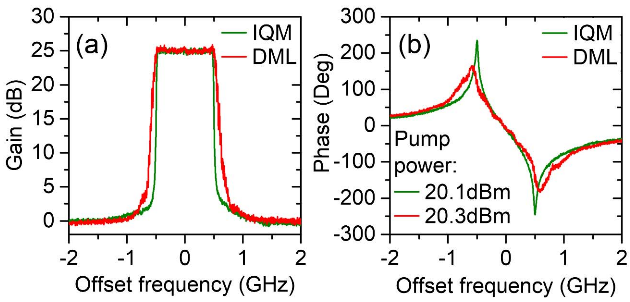

Fig. 6. (a) Amplitude and (b) phase response comparison of the rectangular filters between the DML and IQM approaches.

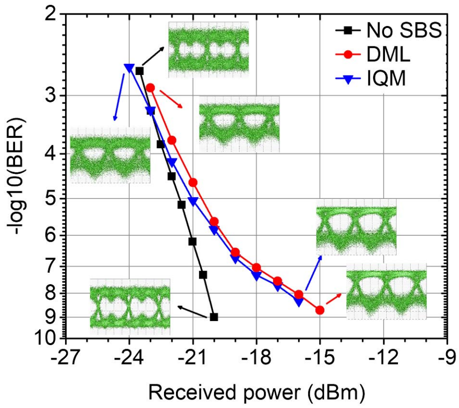

Fig. 7. BER of 500 Mb/s NRZ-OOK signals with and without the MPF.

Funding. National Natural Science Foundation of China (NSFC) (61575122).

REFERENCES

1. J. Yao, J. Lightwave Technol. **27**, 314 (2009).
2. J. Capmany and D. Novak, Nat. Photonics **1**, 319 (2007).
3. V. R. Supradeepa, C. M. Long, R. Wu, F. Ferdous, E. Hamidi, D. E. Leaird, and A. M. Weiner, Nat. Photonics **6**, 186 (2012).
4. S. Xiao and A. M. Weiner, J. Lightwave Technol. **24**, 2523 (2006).
5. B. Vidal, M. A. Piqueras, and J. Marti, Opt. Lett. **32**, 23 (2007).
6. Y. Stern, K. Zhong, T. Schneider, R. Zhang, Y. Ben-Ezra, M. Tur, and A. Zadok, Photon. Res. **2**, B18 (2014).
7. D. Marpaung, B. Morrison, M. Pagani, R. Pant, D. Choi, B. Luther-Davies, S. J. Madden, and B. J. Eggleton, Optica **2**, 76 (2015).
8. L. Yi, W. Wei, Y. Jaouën, M. Shi, B. Han, M. Morvan, and W. Hu, J. Lightwave Technol. **34**, 669 (2016).
9. W. Wei, L. Yi, Y. Jaouën, and W. Hu, Sci. Rep. **6**, 35621 (2016).
10. A. Zadok, A. Eyal, and M. Tur, J. Lightwave Technol. **25**, 2168 (2007).
11. E. Cabrera-Granado, O. G. Calderón, S. Melle, and D. J. Gauthier, Opt. Express **16**, 16032 (2008).
12. L. A. Coldren, S. W. Corzine, and M. L. Masanovic, *Diode Lasers and Photonic Integrated Circuit* (Wiley, 2012).
13. G. P. Agrawal, *Nonlinear Fiber Optics* (Academic, 2010).
14. T. L. Koch and R. A. Linke, Appl. Phys. Lett. **48**, 613 (1986).
15. H. Shalom, A. Zadok, M. Tur, P. J. Legg, W. D. Cornwell, and I. Andonovic, IEEE J. Quantum Electron. **34**, 1816 (1998).
16. J. C. Cartledge and R. C. Srinivasan, J. Lightwave Technol. **15**, 852 (1997).
17. Y. Souidi, F. Taleb, J. Zheng, M. W. Lee, F. D. Burck, and V. Roncin, Appl. Opt. **55**, 248 (2016).
18. W. Wei, L. Yi, Y. Jaouën, M. Morvan, and W. Hu, IEEE Photon. Technol. Lett. **27**, 1593 (2015).